Photolysis of nitric acid in solid nitrogen

WheiJen Chen, WenJui Lo, BingMing Cheng, and YuanPern Lee

Citation: The Journal of Chemical Physics **97**, 7167 (1992); doi: 10.1063/1.463541
View online: http://dx.doi.org/10.1063/1.463541
View Table of Contents: http://scitation.aip.org/content/aip/journal/jcp/97/10?ver=pdfcov
Published by the AIP Publishing

Photolysis of nitric acid in solid nitrogen

Whei-Jen Chen, Wen-Jui Lo, Bing-Ming Cheng,[a] and Yuan-Pern Lee[b]
Department of Chemistry, National Tsing Hua University, 101, Sec. 2, Kuang Fu Road, Hsinchu, Taiwan 30043, Republic of China

(Received 16 June 1992; accepted 7 August 1992)

The large shifts (-30.5 and $+41.7$ cm^{-1}, respectively) of the IR absorption lines of nitric acid ($HONO_2$) in a N_2 matrix in the ν_1 (OH stretching) and ν_3 (HON bending) vibrational modes, relative to those observed for $HONO_2$ in an Ar matrix, indicate a strong interaction between $HONO_2$ and N_2. Photolysis of $HONO_2$ in solid Ar produced predominantly HOONO, whereas relatively intense lines of N_2O and HONO were observed after photolysis of $HONO_2$ in solid N_2 with a mercury lamp, with the relative yield of HOONO decreased by more than a factor of 10. Possible photochemical processes are discussed.

I. INTRODUCTION

The reaction of $OH+NO_2$ to form nitric acid ($HONO_2$)

$$OH+NO_2+M\rightarrow HONO_2+M \qquad (1a)$$

is important in the atmosphere. There has been speculation that peroxynitrous acid (HOONO) might also be formed via a second reaction channel[1,2]

$$OH+NO_2+M\rightarrow HOONO+M. \qquad (1b)$$

However, the search for the IR absorption of HOONO in the gaseous reaction of OH with NO_2 was unsuccessful; when Burkholder *et al.*[3] used a high-resolution Fourier-transform infrared (FTIR) spectrometer coupled with a rapid-flow multipass absorption cell they failed to observe any IR absorption in the range 1850–3850 cm^{-1} that they could ascribe to HOONO.

Recently when we irradiated $HONO_2$ in solid Ar at 12 K with various sources of ultraviolet light we observed IR absorption of HOONO.[4] IR absorption lines at 3545.5, 1703.6, 1364.4, 952.0, and 772.8 cm^{-1} were assigned to various vibrational modes of HOONO on the basis of isotopic shifts. Under certain experimental conditions a second set of lines displaced 5–18 cm^{-1} from the former lines toward greater wave number were also observed; they were attributed to HOONO in a less stable site in the Ar matrix.

The observed vibrational frequencies of ν_1 (OH stretching) and ν_3 (HON bending) of $HONO_2$ in solid Ar, although similar to those in the gas phase, were quite different from those reported previously for $HONO_2$ in solid N_2 by Guillory and Bernstein.[5] These anomalous matrix shifts indicate a strong interaction between $HONO_2$ and N_2. These conditions warrant an investigation whether the photochemistry of $HONO_2$ isolated in solid N_2 differs from that in solid Ar as a consequence of the strong interaction between matrix guest and host. We found that the yield of HOONO was small after photolysis of $HONO_2$ in the N_2 matrix and that there were additional products of photolysis, N_2O and HONO. We report here these observations and compare the photochemistry of $HONO_2$ in solid Ar and N_2.

II. EXPERIMENT

The experimental setup is a typical matrix-isolation/FTIR arrangement described previously.[4] The sample support was a CsI window cooled to 12 K. Windows of KBr and fused silica were mounted on the vacuum shroud along the axes of the IR (probe) and the photolysis beams, respectively. Various photolysis light sources have been employed: a low-pressure Hg lamp, a 100 W medium-pressure Hg lamp, a Nd-YAG laser (266 nm and 355 nm, 10 Hz, Spectra Physics, Model DCR-11 or DCR-2), a XeCl excimer laser (308 nm, 10–50 Hz, Lambda Physik, LPX105), and a KrF excimer laser (248 nm, 10–200 Hz, Lambda Physik, LPX120i). The photolysis radiation was projected from either the same side or the opposite side of the deposition surface. When the photolysis radiation was projected from the opposite side of the deposition surface, the CsI target window served as a filter. We placed proper filters in front of the Hg lamp in order to select the emission of the desired wavelength.

IR absorption spectra of the matrix were recorded before and after irradiation by means of a FTIR spectrometer (Bomem DA3.002) equipped with a KBr beam splitter and a narrow-range Hg/Cd/Te detector cooled with liquid N_2 to cover the spectral range 700–4000 cm^{-1}. Occasionally, a wide-range Hg/Cd/Te detector was used to extend the range to 500 cm^{-1}, although its detectivity is relatively poor. Typically 300–500 scans were collected and the spectral resolution was 0.5 cm^{-1}.

UV absorption spectra were recorded with an optical multichannel analyzer (EG&G, OMAIII with a 1420BR array detector). A deuterium lamp (Hamamatsu, 150W, model L1835) was used as a light source. The emission, passed through a neutral density filter and the matrix sample, was dispersed with a monochromator (Jobin Yvon, HR320) before detection. The reciprocal linear dispersion of the monochromator is 2.5 nm/mm, and the slit width was 40 μm. Each frame of the optical multichannel analyzer (OMA) spectrum covered the wavelength range of

[a]Present address: Synchrotron Radiation Research Center, Hsinchu, Taiwan, R. O. C.
[b]To whom correspondence should be addressed. Also affiliated with the Institute of Atomic and Molecular Science, Academia Sinica, Taiwan, R. O. C.

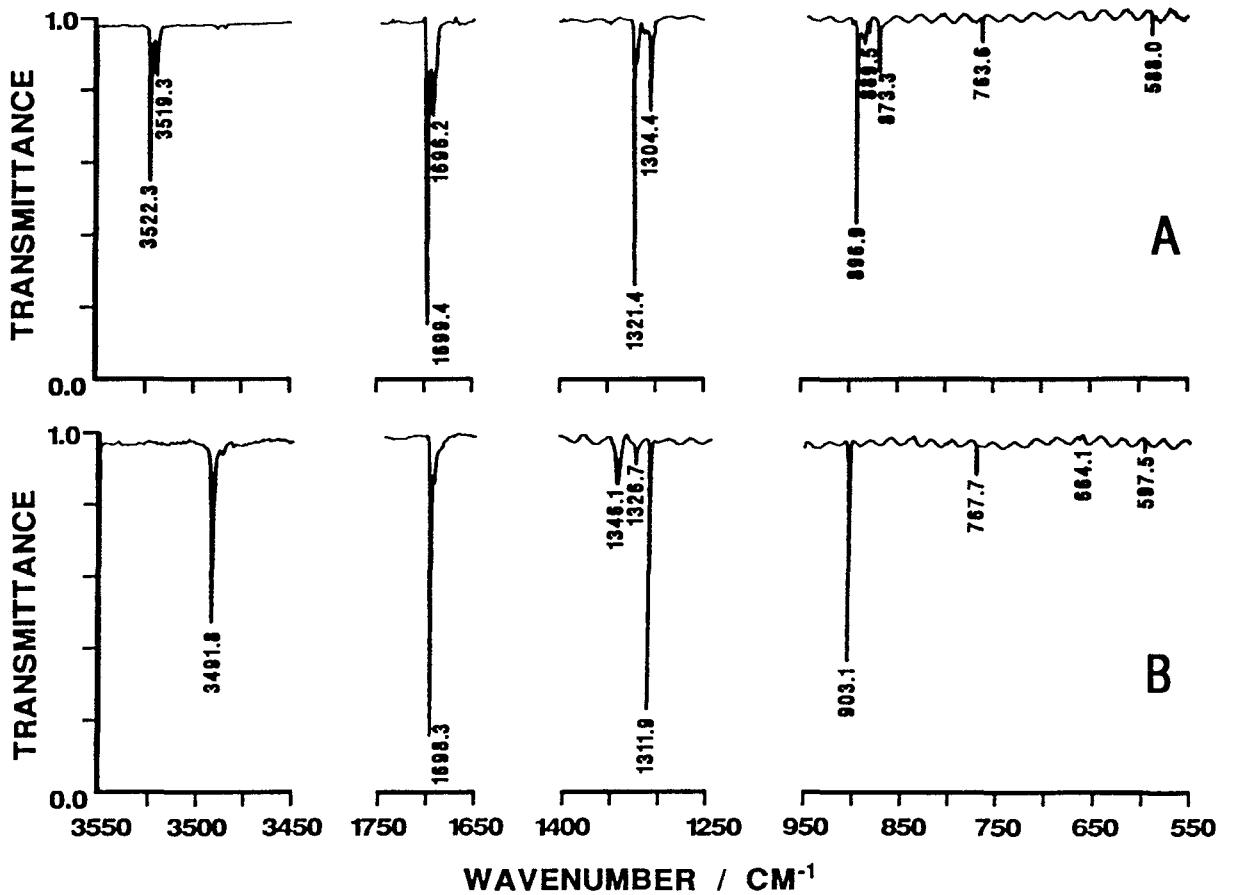

FIG. 1. IR absorption spectra of matrix samples of $HONO_2$/Ar (1/5000, trace A) and $HONO_2/N_2$ (1/5000, trace B).

~43 nm; five frames of the spectra were combined to cover the spectral range 200–400 nm.

The molar fraction of nitric acid in Ar or N_2 was varied from 1/1000 to 1/10000 for IR detection and 1/100 to 1/1000 for UV detection. Typically approximately (4–8) $\times 10^{-3}$ mol of gas mixture was deposited with a flow rate (4–9) $\times 10^{-3}$ mol h^{-1} during a period 30–60 min. In a few experiments, special care was taken to eliminate trace H_2O from the system. However, the experimental results of the matrices with trace H_2O and without H_2O showed no differences.

The various anhydrous isotopic species of $HONO_2$ were prepared by mixing concentrated (98%) sulfuric acid (or deuterated sulfuric acid) with sodium nitrate (99.5%, ^{14}N or ^{15}N species). The product was distilled under vacuum and stored at 195 K in the dark. HONO was prepared by reacting $NaNO_2$ with concentrated sulfuric acid. The isotopic purity of D_2SO_4 and $Na^{15}NO_3$ was 99%. Ar (99.9995%) and N_2(99.999%) were used without further purification.

III. RESULTS AND DISCUSSION

A. IR absorption of $HONO_2$ in Ar and N_2 matrices

The observed IR absorption spectra of three isotopic species of $HONO_2$ isolated in solid N_2 are within experimental uncertainties of those reported previously by Guillory and Bernstein.[5] Figure 1 shows the IR absorption spectra of $HONO_2$ isolated in solid Ar and N_2. The OH-stretching (ν_1) mode shifted from 3522.3 to 3491.8 cm^{-1} whereas the HON-bending (ν_3) mode shifted from 1304.4 to 1346.1 cm^{-1}, as the matrix host was altered from Ar to N_2. Table I compares the fundamental vibrational frequencies of $HONO_2$ in the gas phase,[6–11] in solid N_2, and in solid Ar. The matrix shifts (from the values in the gas phase) for the OH stretching (ν_1) and HON bending (ν_3) are only -27.7 and 1.9 cm^{-1} for the Ar matrix, respectively, whereas the shifts increase to -58.2 (-1.6%) and 43.6 cm^{-1} (3.3%) for the N_2 matrix.

These matrix shifts much exceed what one normally expects for closed-shell molecules isolated in an inert medium.[12] The opposite direction of the shifts for ν_1 and ν_3 suggests that the OH group of $HONO_2$ interacts with another molecule. As the interaction weakens the O–H bond, consequently the vibrational frequency of OH stretching decreases; as it also restricts the motion of the H atom, hence the HON bending frequency increases. The possibility of the formation of dimers of $HONO_2$ in the N_2 matrix, which also give the same trend in the frequency shifts, is eliminated because the spectrum remained constant when the mole ratio was varied from 10^{-3}–10^{-4}. Guillory and Bernstein[5] previously reported a change in vibrational

TABLE I. Vibrational frequencies (in cm^{-1}) of various isotopic nitric acid.

	$HONO_2$				$HO^{15}NO_2$				$DONO_2$			
Assignments	Gas[b]	N_2[c]	N_2[a]	Ar[d]	Gas[b]	N_2[c]	N_2[a]	Ar[a]	Gas[b]	N_2[c]	N_2[a]	Ar[a]
ν_1, HO stretch	3550	3490	3491.8	3522.3 3519.3	3550	3488	3491.5	3522.2 3519.0	2622	2574	2576.5	2601.5 2599.1
ν_2, NO_2 *a* stretch	1709.6[e]	1697	1698.3	1699.4 1696.2	1672	1659	1663.2	1663.8 1660.7	1687	1669	1669.2	1678.6 1674.9
ν_3, HON bend	1302.5[f]	1343	1346.1	1304.4	1321	1339	1341.5	1289.6	1014	1031	1032.4	1013.4 1012.2
ν_4, NO_2 *s* stretch	1325.6[f]	1311	1311.9	1321.4 1318.7	1327	1294	1295.0	1317.5 1314.2	1308	1311	1311.1	1310.4
ν_5, ON stretch	879.1[g]	902	903.1	896.9 889.5	871	892	892.8	888.8 876.6	888	905	906.0	894.2 884.5
ν_6, NO_2 scissors	646.8[h]	660	664.1	656.6	647	658	662.4	[j]	641	660	[k]	[j]
ν_7, ONO_2 in-plane bend	580.3[h]	597	597.5	588.0	578	594	593.5	[j]	541	559	559.9	[j]
ν_8, ONO_2 out-of-plane bend	763.2[h]	767	767.7	763.6	744	746	748.0	744.6	762	767	767.7	763.7
ν_9, HON torsion	458.2[i]	479	[j]	[j]	456	479	[j]	[j]	342	361	[j]	[j]

[a]This work.
[b]Reference 6, unless noted.
[c]Reference 5.
[d]Reference 4.
[e]Reference 7.
[f]Reference 8; ν_3 listed as 1330 cm^{-1} in Ref. 6.
[g]Reference 9.
[h]Reference 10.
[i]Reference 11.
[j]Beyond the detection range of our experiments.
[k]Too weak to be observed.

wave numbers from 3490 to 3280 cm^{-1} for the OH-stretching mode and 1343 to 1398 cm^{-1} for the HON-bending mode when some $HONO_2$ monomers were converted to dimers by diffusion due to warming of the matrix. Hence, we conclude that $HONO_2$ interacts with the N_2 matrix host.

Similar effects are expected for similar molecules such as HONO. For *t*-HONO, the OH stretching shifted from 3590.7 to 3552 cm^{-1} and the HON bending shifted from 1263.2 to 1298 cm^{-1} when the molecule was changed from the gaseous to the N_2–matrix-isolated state.[13–15] Based on the magnitude of the matrix shifts, the interaction between $HONO_2$ and N_2 is relatively weaker than the H bonding in the dimeric $HONO_2$.

The nature of the interaction between $HONO_2$ and the N_2 matrix is not exactly clear on the basis of our experimental results. N_2 matrix is known to have a smaller cage, so that steric effects are greater than that in an Ar matrix; hence the motion of the guest molecules is more restricted in a N_2 matrix than in an Ar matrix. It is also possible that a six-membered ring structure of the $HONO_2 \cdot N_2$ complex exists in the matrix.

(2)

The classical resonance structure indicates that the HO–N bond in $HONO_2$ would be strengthened and the N_2-attached N=O bond weakened as a result of the interaction. With such a constraint of the structure, one would expect that, in addition to the relatively large shifts in ν_1 and ν_3 discussed above, an increase in ν_5 (HO–N stretching), a decrease in ν_4 (NO_2 *s* stretching), and possible increases in ν_6 (NO_2 scissor), ν_7 (ONO_2 in-plane bending), ν_8 (ONO_2 out-of-plane bending), and ν_9 (HON torsion) due to the added strain of motion. Indeed a decrease in ν_4 (-9.5 cm^{-1}) and increases in ν_5–ν_8 (6.2, 7.5, 9.5, 4.1 cm^{-1}) were observed when the matrix host was altered from Ar to N_2.

B. Photolysis of $HONO_2$ in Ar and N_2 matrices

The product of photolysis in a $HONO_2$/Ar matrix with a medium-pressure Hg lamp was predominantly HOONO;[4] weak absorption lines due to OH (3548.1 cm^{-1}), HNO (2715.4 and 1562.2 cm^{-1}), NO_2 (1610.8 cm^{-1}), and NO (1871.7 cm^{-1}) as photolysis products were also observed. The results are shown in trace A of Fig. 2. The line positions of various isotopic HOONO in solid Ar and N_2 are listed in Table II.

When $HONO_2$ in a N_2 matrix was photolyzed with a medium-pressure Hg lamp, HOONO was formed in a relatively small yield, as shown in trace B of Fig. 2. After a comparable amount of $HONO_2$ was decomposed in solid N_2, the yield of HOONO was less than 10% that observed in an Ar matrix. In addition to the weak absorption of

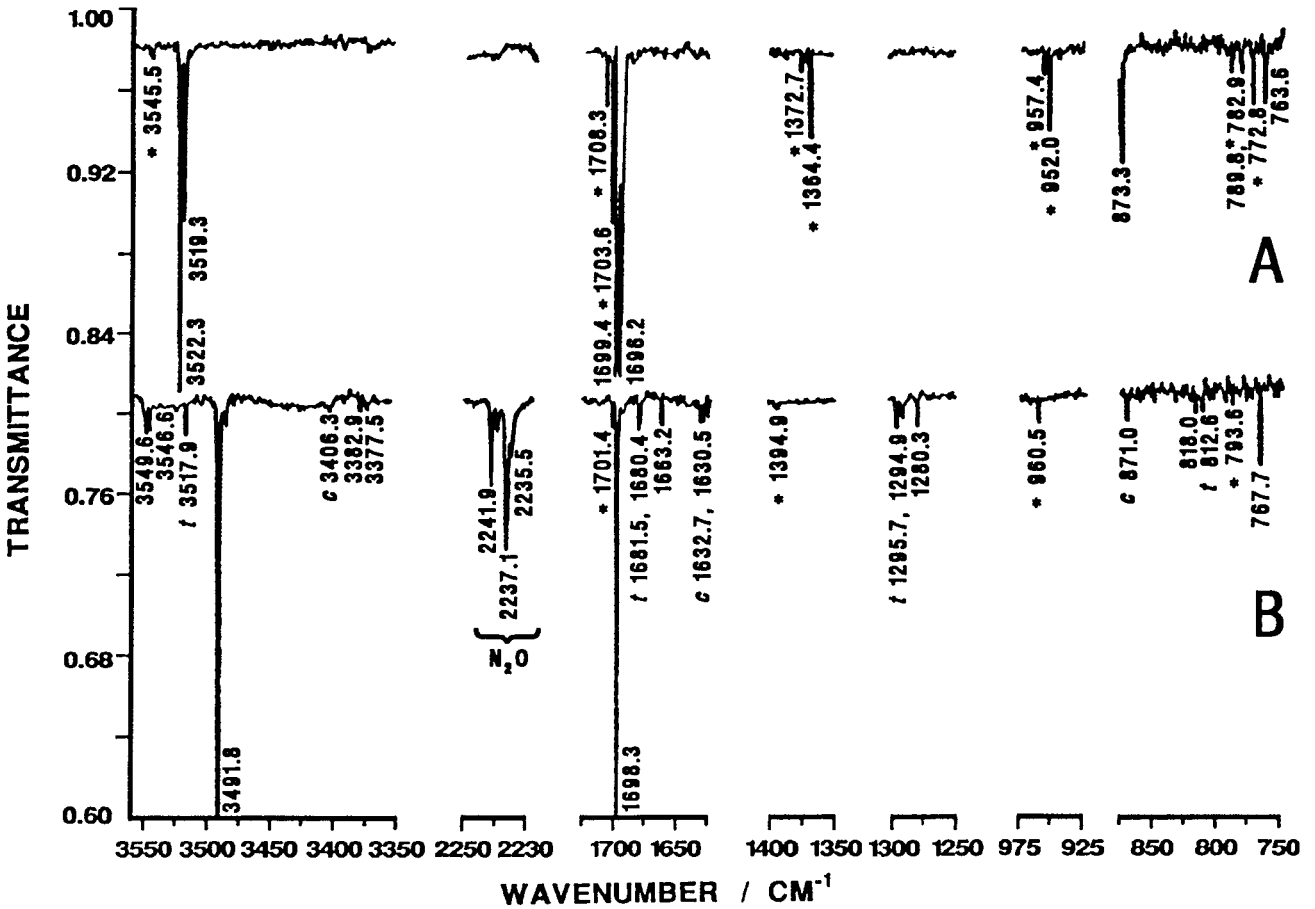

FIG. 2. IR absorption spectra of matrix samples of $HONO_2$/Ar (1/5000, trace A) and $HONO_2/N_2$ (1/5000, trace B) after irradiation with a medium-pressure Hg lamp. The absorption lines are labeled as HOONO (*); *t*-HONO (*t*); *c*-HONO (*c*).

HOONO (marked * in Fig. 2), NO_2 (1616.0 cm^{-1}), OH (3546.6 cm^{-1}), and NO (1874.9 cm^{-1}), relatively intense absorption due to N_2O (2235.5, 2237.1, 2240.1, 2241.9 cm^{-1}), and *t*-HONO (3517.8, 1681.5, 1295.7, 812.6 cm^{-1}, marked *t* in Fig. 2) was also observed after UV photolysis of the $HONO_2/N_2$ matrix. Weak lines due to *c*-HONO (3406.3, 1632.7, 871.0 cm^{-1}, marked *c* in Fig. 2) were also observed in a few experiments.

TABLE II. Comparison of fundamental vibrational frequencies (in cm^{-1}) of various isotopic HOONO in solid Ar and N_2.[a]

	HOONO		$HOO^{15}NO$		DOONO	
Modes	in Ar	in N_2	in Ar	in N_2	in Ar	in N_2
HO stretch	3545.5 (3563.3)[b]	3541.7	3545.7 (3563.4)	3540.7	2615.4 (2633.5)	2622.3
N=O stretch	1703.6 (1708.3)	1701.4	1673.8 (1678.3)	1671.2	1703.7 (1708.3)	1701.8
HOO bend	1364.4 (1372.7)	1394.9	1364.1 (1372.5)	1393.5	1089.7 (1091.7)	1090.7
OO stretch	952.0 (957.4)	960.5	947.7 (953.3)	956.3	950.3 (955.7)	957.3
ON=O bend	772.8 (782.9)	793.6	764.0 (774.0)		772.1 (782.0)	790.3

[a]The ON stretching, ON=O torsional, OON bending, and HOO torsional modes are all below 500 cm^{-1}, beyond our detection limit.
[b]Numbers in parentheses correspond to HOONO in a less stable matrix site.

In order to assign correctly the absorption lines of the products after photolysis, we have also recorded IR absorption spectra of several possible products isolated in solid N_2. The IR spectrum of a N_2O/N_2 (1/5000) matrix showed absorption lines at 1291.1 (ν_1, NO stretching) and 2235.5 (ν_3, NN stretching), in excellent agreement with previous measurements.[16] After the matrix was warmed to approximately 23 K for 10 min, a small absorption line at 2239.8 cm^{-1} was observed, presumably due to aggregates of N_2O. Our observation of a weak line at 2235.5 cm^{-1} after photolysis of a $HONO_2/N_2$ matrix corresponds well with the absorption of isolated N_2O; the more intense lines observed at 2237.1 and 2241.9 cm^{-1} may be due to N_2O perturbed by a nearby molecule.

The IR spectrum of a $HONO/N_2$ (1/1000) matrix

The observed fundamental vibrational frequencies (in cm^{-1}) of various isotopic HOONO in solid Ar and N_2 are compared in Table II. Similar to those observed in $HONO_2$, the wave numbers for the HOO bending and the ON=O bending modes increased substantially as the matrix host was altered from Ar to N_2.

TABLE III. Comparison of the products of photolysis of HNO_3/N_2 matrices from various light sources.[a]

Species	Line /cm^{-1}	Photolytic sources: low-*P* Hg lamp (2 h)	med-*P* Hg lamp (2 h)	KrF 248 nm (1 h 35 min)
OH	3546.6	0.82	0.39	···
NO	1874.9	2.40	0.67	1.20
N_2O	2235.5	1.23	3.10	3.16
HOONO	1701.4	3.70	0.57	···
t-HONO	1681.5	0.90	0.57	···
NO_2	1616.0	2.64	4.16	8.88
Photolysis efficiency[b]		0.17	0.42	0.41

[a]The numbers listed are the ratios of the peak absorbance of the product at the listed wave numbers to the decrease in peak absorbance of $HONO_2$ at 767.7 cm^{-1}.
[b]Fraction of the decrease in peak absorbance of $HONO_2$ at 767.7 cm^{-1}.

showed absorption lines at 3517.8, 1681.1, 1296.3, and 814.4 cm^{-1} due to *t*-HONO and 3406.3, 1630.7, and 871.0 cm^{-1} due to *c*-HONO. The values are within experimental uncertainties of previous reports.[14,15] The line observed at 3517.8, 1681.5, 1295.7, and 812.6 cm^{-1} after photolysis of $HONO_2/N_2$ matrix correspond well to those of the $HONO/N_2$ matrix.

Several photolytic sources other than the Hg lamps have also been tested; no additional features were observed. Table III summarizes the relative peak absorbance of various products of photolysis by different photolytic sources; it may be compared with a similar one (Table III) in the previous report for the photolysis of a $HONO_2$/Ar matrix.[4] Unlike that observed in Ar matrix, photolysis of $HONO_2/N_2$ matrix at 308 nm (XeCl laser) or 266 nm (fourth harmonic of Nd-YAG laser) produced no detectable product. When a medium-pressure Hg lamp was used as a photolysis source, HOONO was observed with a yield approximately 9% that produced in the Ar matrix; relatively intense lines due to NO_2 and N_2O were observed instead. The results are similar except that the yield of HOONO was increased when a low-pressure Hg lamp (254 nm) was used. The spectrum of the $HONO_2/N_2$ matrix sample photolyzed at 248 nm (KrF excimer laser) also showed a relatively small yield of HOONO and relatively intense lines due to N_2O and NO_2, when compared with that of $HONO_2$/Ar.

C. Mechanism of photolysis

In the gas phase, photolysis of $HONO_2$ proceeds via several paths depending on the wavelength[17]

$$HONO_2 \xrightarrow{h\nu} OH + NO_2, \quad D_0 = 2.07 \pm 0.02 \text{ eV}, \tag{3a}$$

$$\xrightarrow{h\nu} O(^3P) + HONO, \quad D_0 = 3.11 \pm 0.01 \text{ eV}, \tag{3b}$$

$$\xrightarrow{h\nu} H(^2S) + NO_3, \quad D_0 = 4.3 \pm 0.3 \text{ eV}, \tag{3c}$$

$$\xrightarrow{h\nu} O(^1D) + HONO, \quad D_0 = 5.08 \pm 0.01 \text{ eV}. \tag{3d}$$

The dissociation energies correspond to wavelengths 599, 399, 288, and 244 nm, respectively, for channels (3a)–(3d). Johnston *et al.*[18] analyzed the end products of photolysis in the range 200–315 nm and reported a quantum yield ~1 for channel (3a). At 266 nm, the quantum yield for the production of O atoms has been determined to be 0.03 by Margitan and Watson.[19] Recently, Vaghjiani and Ravishankara[20] reported quantum yields of 0.95 ± 0.09 for channel (3a) and 0.031 ± 0.010 for channel (3b), with negligible quantum yields for channels (3c) and (3d), for the photolysis of $HONO_2$ at 248 nm. It appears that for $\lambda \geqslant 250$ nm, OH and NO_2 are the only major products in the gas phase.

Photolysis of NO_2 produces O and NO (Ref. 17)

$$NO_2 \xrightarrow{h\nu} O(^3P) + NO, \quad D_0 = 3.12 \pm 0.01 \text{ eV}, \tag{4a}$$

$$\xrightarrow{h\nu} O(^1D) + NO, \quad D_0 = 5.09 \pm 0.01 \text{ eV}. \tag{4b}$$

The dissociation energies in the gas phase correspond to wavelengths 398 and 244 nm for channels (4a) and (4b), respectively. Photolysis of HONO proceeds via[17]

$$HONO \xrightarrow{h\nu} OH + NO, \quad D_0 = 2.09 \pm 0.03 \text{ eV}, \tag{5a}$$

$$\xrightarrow{h\nu} H + NO_2, \quad D_0 = 3.36 \pm 0.03 \text{ eV}. \tag{5b}$$

The dissociation energies in the gas phase correspond to wavelengths 593 and 369 nm for channels (5a) and (5b), respectively.

The photolytic processes of $HONO_2$ in solid Ar are readily deduced. Photolysis of $HONO_2$ at 254 nm yielded predominantly OH and NO_2. The matrix cage effect prevents the separation of some photolyzed pairs; recombination of OH and NO_2 forms both $HONO_2$ and HOONO. Hence, in addition to OH and NO_2, HOONO is the major product of photolysis. Further photolysis of NO_2 produces NO. The small amount of HONO observed in the experiments may result from the reaction of OH with NO.

As the photolytic processes of $HONO_2$ in solid N_2 differ from those in solid Ar, the observed products differ. An increased threshold of photolysis and a decreased yield of HOONO were observed. Furthermore, relatively intense lines due to NO_2, N_2O, and HONO were detected. The decreased yield of HOONO in the N_2 matrix is rationalized by the hypothesis that the OH photofragment in solid N_2 may move less freely than in solid Ar because of its strong interaction with the N_2 matrix; hence it is relatively more difficult to form HOONO than $HONO_2$ because the OH radical must travel further in order to attack the O atom of NO_2 so to form HOONO. The increased photolysis threshold for the production of HOONO is also consistent with such a scheme; the OH fragment in solid N_2 needs more

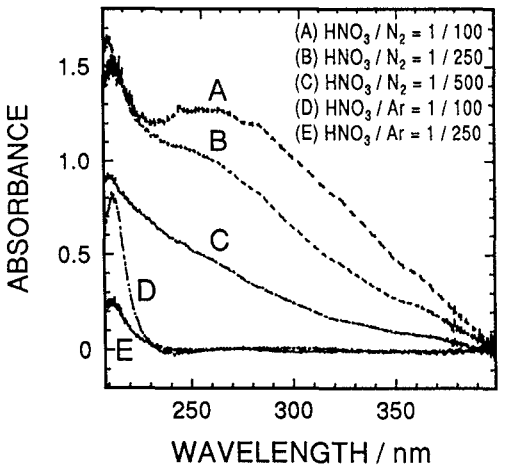

FIG. 3. UV absorption spectra of matrix samples of $HONO_2/N_2$ (1/100, 1/250, and 1/500, trace A–C) and $HONO_2/Ar$ (1/100 and 1/250, trace D and E).

excess energy after photolysis than that in solid Ar in order to overcome the binding from the nearby N_2 host and to move around to form HOONO.

The observation of N_2O as a product of photolysis suggests that $O(^1D)$ was formed. $O(^1D)$ reacts readily with N_2 to form N_2O,[21]

$$O(^1D)+N_2 \rightarrow N_2O \qquad (6)$$

whereas $O(^3P)$ does not react with N_2 in matrix due to symmetry correlation. There are two possible sources of $O(^1D)$: the secondary photolysis of NO_2 [reaction (4b)] or the direct photofragmentation of $HONO_2$ [reaction (3d)]. We have also studied the photolysis of NO_2 in solid N_2; when the matrix sample containing NO_2/N_2 (1/25 000) was irradiated with a low-pressure Hg lamp which emitted mainly at 254 nm, neither N_2O nor NO was detected. These products were observed when the sample was irradiated with a medium-pressure Hg lamp or a KrF laser (248 nm). In contrast, photolysis of the $HONO_2/N_2$ matrix with a low-pressure Hg lamp produced a substantial proportion of N_2O, among other products listed in Table III. The results indicate that at 254 nm the observed photolysis product N_2O did not result from secondary photolysis of NO_2; therefore, the most likely source of $O(^1D)$ is the direct photolysis of $HONO_2$, reaction (3d). The increased yield of HONO also supports that channel (3d) occurred. The formation of the N_2O/HONO pair is similar to the reported formation of the H_2CO/HNO pair in the photolysis of a H_3CONO/Ar matrix.[22,23]

The threshold energy for the production of $O(^1D)$ from photolysis of $HONO_2$ in the gaseous phase is 5.08 eV (corresponding to 244 nm), slightly greater than the 4.88 eV of the 254 nm photons. As the interacted N=O bond in $HONO_2$ may be weakened, and as the excited states are normally more stabilized than the ground state by the matrix interaction, the threshold energy for channel (3d) in solid N_2 may be decreased to below 4.88 eV.

To investigate further this problem, we have measured the UV absorption spectra of $HONO_2$/Ar and $HONO_2/N_2$ matrices at various concentrations, as shown in Fig. 3. To minimize the interference due to the scattering of the matrix, the absorption spectra of pure matrix hosts have been subtracted from those of the matrices containing $HONO_2$. Absorption spectra at ratios of $HONO_2/Ar=1/100$ and 1/250 are shown in traces D and E of Fig. 3; the spectra are similar except that the absorbance changes with the concentration of $HONO_2$. The absorption spectrum of $HONO_2$ in solid Ar is similar to that observed in the gas phase. Absorption spectra at ratios of $HONO_2/N_2=1/100$, 1/250, and 1/500 are shown in traces A–C of Fig. 3. The increased background absorption throughout the 200–400 nm region indicates that the N_2 lattice changed substantially when $HONO_2$ was present. In addition, an absorption band in the region 240–300 nm which increases with the concentration of $HONO_2$ was observed. This effect further supports our conclusion that N_2 interacts with $HONO_2$ and that the dissociation threshold of $HONO_2$ [to form $O(^1D)$] is decreased in solid N_2 due to the interaction.

In summary, the interaction between $HONO_2$ and N_2 host has a great effect on the photolytic processes of $HONO_2$ induced by UV light. The decreased yield and the increased threshold for the formation of HOONO suggests that the interaction between $HONO_2$ and N_2 host restricts the motion of the OH photofragments. Furthermore, the relatively intense lines due to N_2O [from reaction of $O(^1D)$ with N_2] and HONO which were not observed in a photolyzed $HONO_2$/Ar matrix suggests that the interaction also decreases the photodissociation threshold of the photolytic channel $HONO_2 \rightarrow O(^1D)+HONO$.

ACKNOWLEDGMENT

We thank the National Science Council of the Republic of China for support of this research (Contract No. NSC81-0417-M-007-02).

[1] J. S. Robertshaw and I. W. M. Smith, J. Phys. Chem. **86**, 785 (1982).
[2] R. Atkinson, W. P. L. Carter, and A. M. Winer, J. Phys. Chem. **87**, 2012 (1983).
[3] J. B. Burkholder, P. D. Hammer, and C. J. Howard, J. Phys. Chem. **91**, 2136 (1987).
[4] B.-M. Cheng, J.-W. Lee, and Y.-P. Lee, J. Phys. Chem. **95**, 2814 (1991).
[5] W. A. Guillory and M. L. Bernstein, J. Chem. Phys. **62**, 1058 (1975).
[6] G. E. McGraw, D. L. Bernitt, and I. C. Hisatsune, J. Chem. Phys. **42**, 237 (1965).
[7] A. G. Maki, J. Mol. Spectrosc. **127**, 104 (1988).
[8] A. Perrin, O. Lado-Bordowsky, and A. Valentin, Mol. Phys. **67**, 249 (1989).
[9] A. G. Maki and J. S. Wells, J. Mol. Spectrosc. **108**, 17 (1984).
[10] A. G. Maki and W. B. Olson, J. Mol. Spectrosc. **133**, 171 (1989).
[11] A. Goldman, J. B. Burkholder, and C. J. Howard, J. Mol. Spectrosc. **131**, 195 (1988).
[12] M. E. Jacox, J. Mol. Spectrosc. **113**, 286 (1985).
[13] G. E. McGraw, D. L. Bernitt, and I. C. Hisatsune, J. Chem. Phys. **45**, 1392 (1966) and references therein.
[14] P. A. McDonald and J. S. Shirk, J. Chem, Phys. **77**, 2355 (1982).
[15] R. T. Hall and G. C. Pimentel, J. Chem. Phys. **38**, 1889 (1963).

[16] J. R. Sodear and R. Withnall, J. Phys. Chem. **89**, 4484 (1985).
[17] H. Okabe, *Photochemistry of Small Molecules* (Wiley, New York, 1978).
[18] H. S. Johnston, S.-G. Chang, and G. Whitten, J. Phys. Chem. **78**, 1 (1974).
[19] J. J. Margitan and R. T. Watson, J. Phys. Chem. **86**, 3819 (1982).
[20] A. A. Turnipseed, G. L. Vaghjiani, J. E. Thompson, and A. R. Ravishankara, J. Chem. Phys. **96**, 5887 (1992).
[21] W. B. DeMore and N. Davidson, J. Am. Chem. Soc. **81**, 5869 (1959).
[22] M. E. Jacox and F. L. Rook, J. Phys. Chem. **86**, 2899 (1982).
[23] R. P. Müller, P. Russegger, and J. R. Huber, Chem. Phys. **70**, 281 (1982).